Inorganic Chemistry

Article

pubs.acs.org/IC

$Sr_7Co_4(CO_3)O_{13-\delta}$ (δ = 1.64), An Original Cobaltite Derivative of the Ruddlesden–Popper Series

A. Demont,[†] D. Pelloquin,*[,†] S. Hébert,[†] M. Hervieu,[†] J. Höwing,[‡] and A. Maignan[†]

[†]Laboratoire CRISMAT, UMR CNRS-ENSI Caen 6508, 6 bd Maréchal Juin, 14050 Caen Cedex, France

[‡]Instituttveien 18, 2007 Kjeller, Norway

Supporting Information

ABSTRACT: The oxycarbonate $Sr_7Co_4(CO_3)O_{11.36}$ exhibits a peculiar structure that has been characterized by combining transmission electron microscopy analyses and neutron diffraction. It consists of a regular intergrowth between the m = 2 and carbonated m = 3 members of the $Sr_{m+1}Co_mO_{3m+1}$ Ruddlesden–Popper (RP) series, $Sr_3Co_2O_{5.87}$ and $Sr_4Co_2(CO_3)O_{5.49}$, respectively. A description of the structure is proposed to provide identification of the different building blocks. This material is semiconducting and presents a complex magnetic behavior, characteristic of what is observed for the RP^2 or RP^3 series, with a cobalt valency close to 2.7.

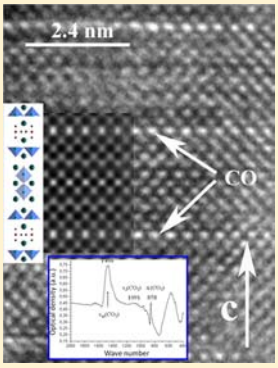

INTRODUCTION

The discovery of Sr_2TiO_4 and $Sr_3Ti_2O_7$ by Ruddlesden and Popper[1] 50 years ago has opened a door toward a wide family of compounds that are members of the $(SrO)^{RS}(SrTiO_3)^{P}_m$ series (RS for rock salt and P for perovskite). The large chemical and structural flexibility of these structures provides access to a great tunability of the chemical and physical properties, which can be compared with those of perovskite. The RP family was later enlarged with the formation of derivative series $(AO)^{RS}_n(A'MO_3)^{P}_m$,[8−20] commonly referred to as RP^n_m compounds or simply described by four numbers, $[(n-1)\ 2\ (m-1)\ m]$. Variation of the relative n and m numbers, as well as the structure of the different layers with $[Ln_2O_2]$ fluorite-type layers[2] and $[Bi_2O_{2+\delta}]$ layers,[3] or the introduction of various polyanions such as carbonate, nitrate, chromate, or sulfate groups[4−7] led to a huge diversity of RP derivatives, enabling the possible stabilization of complex intergrowths. Such a potential makes the RP series a preponderant class of materials, involved in promising applicative fields such as colossal magnetoresistance in the manganites[21] or high T_c superconducting properties in the cuprates.[24,25]

In numerous RP^1_m families, the 0223 compound (RP^1_3) is the limit single-phase member. Moreover, regular intergrowths of RP^1_m and $RP^1_{m'}$ have so far never been reported in the RP^1_m series despite extensive studies of the RP systems through the variation of A, A′, and M. Owing to the possibility of carbonate and hydroxyl group incorporation in perovskite-related blocks, two novel layered structures, $Sr_4Co_2(CO_3)O_{6-\delta}$ and $Sr_4Co_{2.3}(CO_3)_{0.7}O_{6-\delta}(OH)_2$,[22,23] were recently isolated whose structures are associated with that of the ideal RP^1_3 member $Sr_4Co_3O_{10}$. In both structures, the intermediate layer of the triple perovskite block $[Sr_3Co_3O_9]_\infty$ is replaced by a carbonated $[SrCO_2]$ layer (denoted "SC" herein), as was previously observed in the superconducting intergrowth $TlSr_2CuO_5$ or $Bi_2Sr_2CuO_6/Sr_2Cu(CO_3)O_2$ (denoted as 1201/S_2CC or 2201/S_2CC, respectively),[24,25] whereas (OH^-) hydroxyl groups replace O ions in RS-type [SrO] layers, following a mechanism previously observed in the derivative RP^1_2 cobaltite.[26] Clearly, such substitutions/intergrowths change the magnetic behavior, leading to superconducting properties[24] or a ferromagnetic component.[26]

In this paper, we report the synthesis and study of a new complex oxycarbonate characterized by a large oxygen nonstoichiometry, $Sr_7Co_4(CO_3)O_{13-\delta}$ with δ = 1.64. Its crystal chemistry was studied using electron (ED), X-ray (XRD), and neutron (ND) diffraction, IR spectroscopy, and high-resolution transmission electron microscopy (TEM). Its structure consists of a regular intergrowth between the RP^1_2 and carbonated RP^1_3 frameworks. More generally, this original layered compound can be described as the first example of highly ordered intergrowth between three distinct structural units, namely, RP^1_2, RP^1_1, and S_2CoC. Its electrical transport and magnetic behavior are also presented.

EXPERIMENTAL SECTION

Taking into account TEM, energy-dispersive spectroscopy (EDS), and XRD early analyses in $Sr_4Co_{3-x}(CO_3)_xO_{10-4x-\delta}$ compounds,[22] syntheses were carried out with a Sr/Co ratio in the vicinity of ∼7/4. In order to isolate the compound, several nominal oxygen and carbonate contents were tested through various relative proportions of SrO and $SrCO_3$. Polycrystalline samples were synthesized by mixing

Received: November 30, 2012
Published: April 5, 2013

   dx.doi.org/10.1021/ic3026232 | Inorg. Chem. 2013, 52, 4977−4984

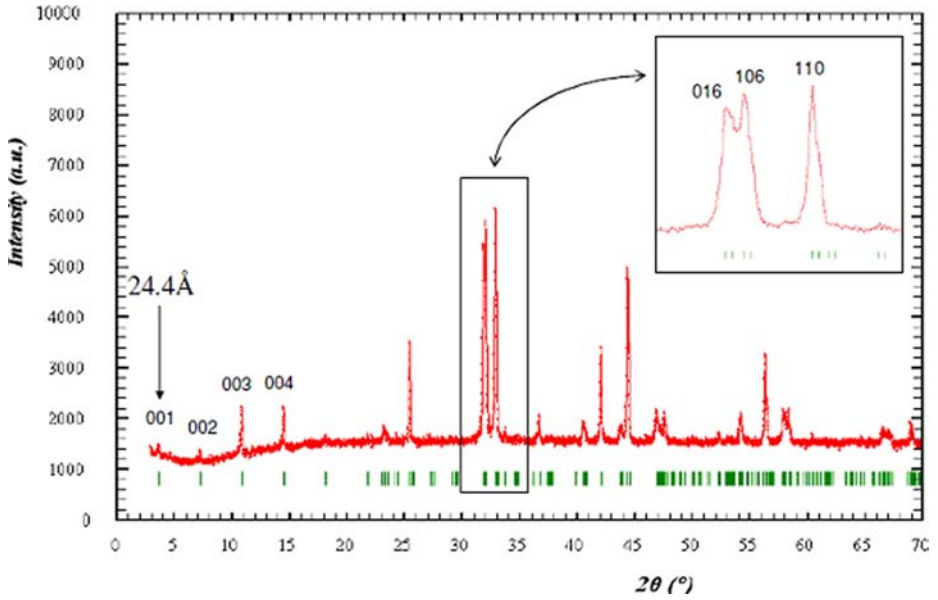

Figure 1. Experimental powder XRD pattern of an as-synthesized $Sr_7Co_4(CO_3)O_{11.36}$ sample. The indexation given in the inset is related to the orthorhombic (3.84 × 3.85 × 24.39 Å^3) cell.

SrO, $SrCO_3$, and Co_3O_4 in proportions of 6:1:4/3. SrO was calcined at 1473 K and introduced while still incandescent in a nitrogen-filled glovebox to be intimately ground with the other precursors and pressed as bars. These bars were introduced into alumina crucibles with a circular section and placed in quartz sealed tubes under a primary vacuum. Black ceramic bars were collected after heating at 1123 K for 24 h and quenching to room temperature. Owing to the reactivity of the related cobalt oxycarbonates,[22] the as-synthesized powder was divided into small parts, kept in sealed capillary glass tubes, and opened shortly before different analyses.

Phase identification was performed with a Panalytical X-Pert Pro diffractometer equipped with an X'Celerator detector and working with Cu Kα radiation. Selected area electron diffraction (SAED) was collected with a JEOL 2010 transmission electron microscope equipped with an EDS INCA analyzer. IR spectroscopy was performed with a Nicolet instrument to check for the presence of carbonates in the sample. High-resolution TEM (HRTEM) was carried out with a JEOL 2011F microscope working with a field emission gun (Cs = 1 mm) and also equipped with an EDS analyzer (EDAX). The ND experiment took place in Kjeller (Norway), on the PUS diffractometer. The corresponding data set was analyzed by the Rietveld method using *WinPlotr* software.[27] Finally, magnetic measurements were performed with a Quantum Design SQUID magnetometer, and the resistivity of the sample was collected by the four-probe method with the transport option of PPMS set up.

RESULTS

Starting from the nominal composition $Sr_7Co_4(CO_3)O_{11.33}$, a single-phase sample is reproducibly obtained (Figure 1), which is unstable under an ambient atmosphere and tends to slowly amorphize when exposed in air, over a several month time scale. The presence of carbonate groups in the crystal structure was confirmed by IR spectroscopy, as shown by the presence of the $\nu_{as}(CO_3)$ and $\nu_s(CO_3)$ characteristic bands in the enlarged part of the spectrum (Figure 2). Moreover, the existence of the $\pi(CO_3)$ band at 858 cm^{-1} shows that the carbonate groups are incorporated in the heart of crystallites.

Diffraction Analyses. ED reconstruction of the reciprocal space was obtained by tilting along the crystallographic axes. The arrangement of the intense reflections leads to a unit cell with $a \sim a_p$, $b \sim a_p$, $c \sim 24$ Å, and $\alpha = \beta = \gamma = 90°$ ($a_p \sim 3.8$ Å

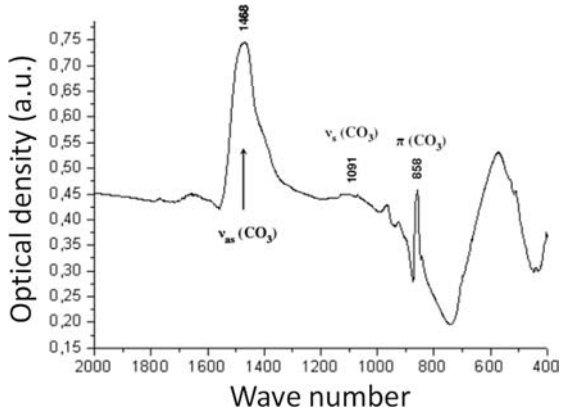

Figure 2. Experimental IR data collected from a freshly as-synthesized $Sr_7Co_4(CO_3)O_{11.36}$ sample.

is the cell parameter of the perovskite unit cell) and no condition limiting the reflection, yielding *Pmmm*, *Pmm*2, and *P*222 as possible orthorhombic space groups. Three typical ED patterns, [010], [1$\bar{1}$0], and [$\bar{1}$30], are presented in Figure 3. The cell parameters were refined from powder XRD patterns (pattern-matching mode) in an orthorhombic cell with a = 3.8438 (5) Å, b = 3.8551 (3) Å, and c = 24.390 (1) Å.

The intensities of the reflections along c^* follow the sequence [one intense - four less - one intense - six less] (Figure 3b,c). In a first approach, this arrangement suggested that the structure is based on the intergrowth of two layered systems.[28] According to the hypothesis of the formation of RP^n_m derivatives (a, $b \sim a_p$; long c axis), with an intergrowth parameter $c \sim nc_{NaCl} + mc_P = 24.4$ Å (with $c_{NaCl} \sim 2.8$ Å, the thickness of one NaCl-type layer, and $c_P \sim 3.85$ Å), the n and m values are consistent with 2 and 5, respectively, in agreement with the cation ratio. With respect to the introduction of carbonates in the framework, the periodicity along $\vec{c}$ ($c \sim 24.4$ Å) was then associated with a regular alternation of the RP^1_2 and carbonated RP^1_3 layered frameworks (see also the SI, sections 1 and 2, for a more complete description).

dx.doi.org/10.1021/ic3026232 | *Inorg. Chem.* 2013, 52, 4977−4984

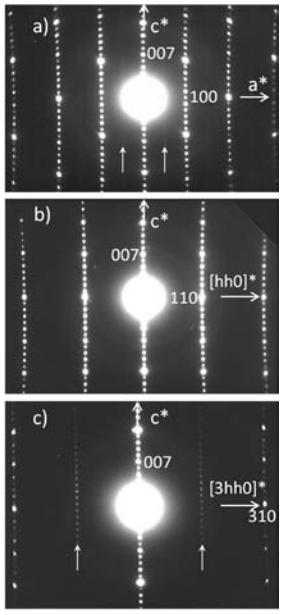

Figure 3. Experimental ED patterns recorded along (a) [010], (b) [1$\bar{1}$0], and (c) [$\bar{1}$30] zone axes, respectively. Extra dots are shown by white arrows.

The [*hk*0] ED patterns (Figure 3a–c) of the freshly prepared samples exhibit sharp reflections, without additional spots or diffuse streaks along *c**, which attest to a regular stacking mode of the two blocks along this axis, with few intergrowth defects. This fits well with the sharpness of the 00*l* reflections observed by powder XRD (see the SI, section 3). Extra spots were detected over the course of the ED study, scarcely visible in the [010]-oriented ED pattern (Figure 3a) and weak but sharp in the [$\bar{1}$30]-oriented pattern (Figure 3c). In the former, diffuse streaks, at $h/2$ running along a reciprocal direction parallel to *c** (white arrows), involve a local doubling of the *a* parameter, which can be interpreted as a local superstructure in the layer plane, with a loss of ordering along the perpendicular direction. However, the sharp satellites along $\vec{c}$ = [310]* involve a doubling of the periodicity compatible with the diffuse line detected in Figure 3a (white arrows). Such an effect has been previously reported[29,30] and directly associated with the existence of a carbonated "C"-type layer (see also the SI, section 4, for more detailed explanations).

First Model from TEM Imaging. HRTEM usually proves to be an efficient tool to visualize the layer stacking of complex materials and locate carbonate groups in such frameworks.[28−32] The lightness of carbon, with respect to strontium and cobalt, combined with highly covalent C−O bonding generates significantly distinctive contrasts for carbonates incorporated in a host RP^n_m matrix. The HRTEM study was mainly carried out along the [100] zone axis, which allows one to visualize clearly the stacking mode. Figure 4 shows wide areas of crystallites with the periodic repetition of distinctively bright contrasts every 24.4 Å (black arrows), as expected for the regular alternation of the RP^1_2 and carbonated RP^1_3 layered frameworks. This peculiar contrast is not observable anymore a few minutes after the beginning of the focus series image recording, illustrating the poor stability of this layered structure under an electron beam. The enlarged HRTEM image presented in Figure 5 has been collected with a defocus value close to 10 nm and shows significantly altered crystallinity on its lower and upper parts. Nevertheless, the central part of this

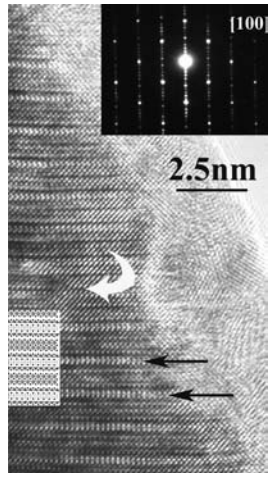

Figure 4. Experimental [100] HRTEM images of wide areas of the crystallite showing the periodic repeat of brighter contrasts (black arrows) correlated with carbonates incorporated into the host RP matrix. Local disturbance is viewed at the level of the white arrow because of the instability of the structure under the electron beam.

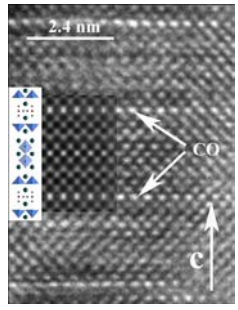

Figure 5. Experimental [100] HRTEM image of the $Sr_7Co_4(CO_3)O_{11.36}$ sample. The corresponding structural model and calculated image (focus value of 10 nm and a thickness ranging from 3.5 to 5 nm) are inserted.

one allows identification of the characteristic contrasts associated with the carbonates (white arrows) sandwiched between two $[SrO]_\infty$ layers.

A first approximation of the model can be proposed, accounting for the XRD and ED data combined with these HRTEM images. The carbonated groups are incorporated in a RP host matrix, where they replace CoO_x polyhedra in the center of a triple perovskite block, as observed in the cobaltite $Sr_4Co_2(CO_3)O_{5.86}$[22] or the ferrite $Sr_4Fe_2(CO_3)O_6$.[33−35] From the HRTEM image shown in Figure 5, the stacking sequence of the layers along $\vec{c}$ can be deduced as [RS-P-P-RS-P-SC-P] with RS for $[SrO]_\infty$, P for $[SrCoO_{3-x}]_\infty$, and SC for $[SrCO_2]_\infty$ layers. Thus, the following developed formulation of a regular intergrowth $[Sr_3Co_2O_{7-\varepsilon}]^{RP_2}[Sr_4Co_2(CO_3)O_{6-\varepsilon'}]^{RP_3}$ can be proposed as inserted in Figure 5.

Powder ND. An accurate study of the stacking mode deduced from TEM observations was carried out using powder ND data in order to investigate the actual oxygen stoichiometry and the carbonate configurations. This model (inset in Figure 5) was introduced in the *FULLPROF* routine implemented in the *WinPlotr* software.[27] Rietveld refinements were performed based on the *Pmmm* space group. A first set of calculations provided the Sr, Co, C, and O atomic positions, except for the O atoms belonging to carbonate groups, according to the [RS-P-P-RS-P-SC-P] sequence. At this stage, Fourier difference

dx.doi.org/10.1021/ic3026232 | *Inorg. Chem.* 2013, 52, 4977−4984

maps were calculated around C atoms (Figure 6). The intensities on these maps were not totally well-defined. It is

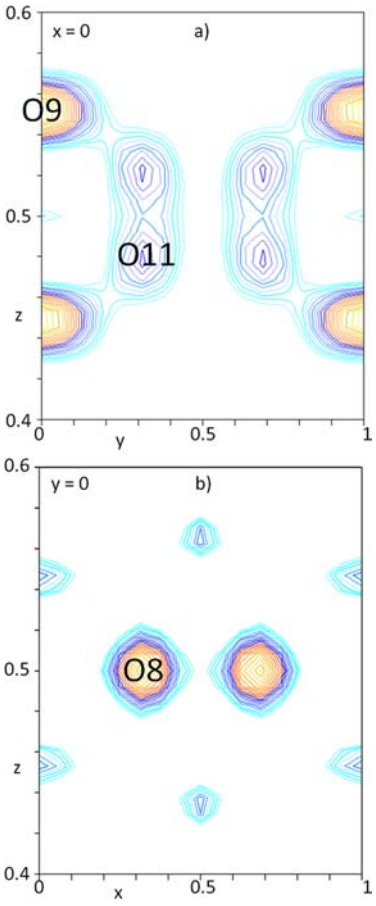

Figure 6. Fourier difference map calculated around C at different stages of the refinement to provide successive detections of O atoms from the carbonates. The C location is (0 0 0.5): (a) location of O9 and O11; (b) location of O8.

then necessary to translate the partial occupancy of O atoms on high-multiplicity sites and to introduce two configurations for triangular CO_3 groups, with O positions extremely close to one another in the average unit cell. From the refined atom coordinates, two configurations were found for the carbonates groups in the structure, coat-hanger (Figure 7b) and flag (Figure 7c), in the same manner as the results reported in refs 30 and 33−36. Given the proximity of these three O sites (Figure 7a) and the possible orientations of the CO_3 triangles, their thermal agitation parameters were constrained to be refined to equal values. The fraction of each configuration was constrained with respect to the global content of one carbonate group per unit cell. The refinements led to 50% of each configuration within the standard deviation range (Figure 7b,c), showing that none of them is clearly favored, as previously observed in other RP derivative oxycarbonates.[33−35] Final refinements were therefore performed considering the coexistence of the two types of configuration. Corresponding structural parameters and final reliability factors are presented in Table 1, and the principal interatomic distances are summarized in Table 2. Observed, calculated, and difference profiles are presented in Figure 8. A theoretical HRTEM [100] image has been calculated from these final atomic positions and superimposed with the experimental one in Figure 5: it fits well

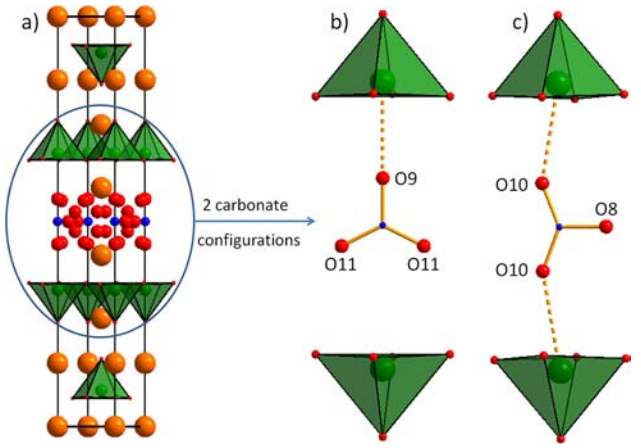

Figure 7. (a) Structural model of the $Sr_7Co_4(CO_3)O_{11.36}$ sample and both limit CO_3 configurations (b and c).

and especially highlights a peculiar row of bright spots every 24 Å (white arrows) that are correlated to the positions of oxygen O8 and C atoms of the carbonate groups.

Structural Discussion. From the ND results, the actual chemical formula of the new compound is $Sr_7Co_4(CO_3)O_{11.36}$, with $Sr_3Co_2O_{5.87}$ for the RP^1_3 block and $Sr_4Co_2(CO_3)O_{5.49}$ for the carbonated RP block, in perfect agreement with the nominal content. The oxygen deficiency of the RP^1_2 block is comparable to that observed in reported parent oxygen-deficient $Sr_3Co_2O_{7-\delta}$ compounds.[37−39] These materials are indeed capable of sustaining a great range of oxygen nonstoichiometry with $0.41 \leq \delta \leq 1.64$. Interestingly, the oxygen vacancies are not statistically distributed but mainly concentrated in the strontium layer stacked between two cobalt layers in the center of the RP^1_2 block, leading to slightly deficient $[CoO_{1.75}]$ layers and strongly deficient $[SrO_{0.38}]$ layers (Figure 9a). The composition deduced from ND analysis yields in an average oxidation state of 2.68+ for cobalt. From bond-valence calculations, Co1 (RP^1_2) and Co2 (carbonated RP^1_3 block) exhibit similar state valences, showing that no charge ordering occurs within one block with respect to the other.

In the carbonated RP^1_3 block, two configurations were found for the carbonate groups in the structure, coat-hanger and flag, in the same way as the results reported in ref 33. Co2 is present in square-based pyramidal environments with two orientations, one with a horizontal basal plane (parallel to the layers) and one with a vertical basal plane (perpendicular to the layers). The respective proportions of these two configurations are 49 and 51% (Figure 7b,c).

The actual $O_{5.87}$ oxygen stoichiometry in the RP^1_2 block yields in an average coordination number of 4.87 for Co2 (Figure 9a). The predominant polyhedra are therefore CoO_5 square-based pyramids, which can be oriented parallel either to the basal plane or to the *c* axis, given the repartition of oxygen vacancies. Two limit configurations can be established from these two distinct environments, which are presented in parts b and c of Figure 9, respectively. Note that the repartition of vacancies along *b* in the second configuration induces the orthorhombic distortion and that both would result in ideal $Sr_3Co_2O_6$ stoichiometry. Both configurations were reported in pure RP^1_2 cobaltites: $Sr_3Co_2O_{6.06}$[37] for the first one and $Sm_2BaCo_2O_6$[40] for the second. One can expect that none of these configurations is favored at high temperature in the present $Sr_7Co_4(CO_3)O_{11.36}$ compound, with a high degree of disorder

dx.doi.org/10.1021/ic3026232 | Inorg. Chem. 2013, 52, 4977−4984

Table 1. Structural Parameters Extracted from Rietveld Analysis of Powder ND Data for $Sr_7Co_4(CO_3)O_{11.36}$[a]

atom	site	x	y	z	B (Å^2)	n
Sr1	1a	0	0	0	0.6(2)	1
Sr2	2q	0	0	0.1545(3)	0.88(17)	2
Sr3	2t	0.5	0.5	0.2642(4)	2.34(19)	2
Sr4	2t	0.5	0.5	0.4179(4)	2.6(3)	2
Co1	2t	0.5	0.5	0.0883(9)	1.0(5)	2
Co2	2q	0	0	0.3335(8)	0.7(4)	2
O1	1f	0.5	0.5	0	1.5(1)	0.38(4)
O2	2r	0	0.5	0.0728(9)	0.1(4)	1.49(11)
O3	2s	0.5	0.0	0.0692(11)	4.4(6)	2[c]
O4	2t	0.5	0.5	0.1649(4)	1.01(16)	2[c]
O5	2q	0	0	0.2543(4)	0.63(13)	2[c]
O6	2s	0.5	0	0.3468(8)	1.9(4)	2[c]
O7	2r	0.0	0.5	0.3502(10)	0.7(4)	1.49(7)
C	1c	0	0	0.5	0.42(18)	1
O8	2j	0.357(15)	0	0.5	2.0(4)[b]	0.50(3)
O9	2q	0	0	0.555(3)	2.0(4)[b]	0.50(3)
O10	4w	0.127(10)	0	0.551(2)	2.0(4)[b]	1.00(3)
O11	4u	0	0.306(9)	0.5241(15)	2.0(4)[b]	1.00(3)

[a] *Pmmm*; a = 3.84383(5) Å; b = 3.85506(3) Å; c = 24.3903(1) Å. R_{wp} = 4.96%; R_p = 3.93%; R_{exp} = 4.04%; χ^2 = 1.51; R_{Bragg} = 3.70%. Phase 2: $Sr_4Co_2(CO_3)O_{5.86}$. [b] Constrained to be equal because of the extreme proximity of O8, O9, O10, and O11 to one another. [c] From top to bottom in the table: respectively 2.08(15), 2.05(5), 1.97(4), and 2.04(13) when refined.

Table 2. Interatomic Distances in $Sr_7Co_4(CO_3)O_{11.36}$

Bond Distances (Å) and Angles (deg)			
Sr1−O1×1.52(16)	2.72196(2)	Co1−O1×0.38	2.15(2)
Sr1−O2×2.98(22)	2.622(15)	Co1−O2×1.49(11)	1.957(6)
Sr1−O3×4	2.561(18)	Co1−O3×2	1.981(8)
		Co1−O4×1	1.87(4)
Sr2−O2×1.49(11)	2.771(17)		
Sr2−O3×2	2.83(2)	Co2−O5×1	1.93(2)
Sr2−O4×4	2.7335(11)	Co2−O6×2	1.951(5)
Sr2−O5×1	2.432(12)	Co2−O7×1.49(7)	1.971(6)
		Co2−O9×0.25(2)	2.75(8)
Sr3−O4×1	2.422(14)	Co2−O10×0.50(2)	2.86(5)
Sr3−O5×4	2.7327(12)		
Sr3−O6×2	2.794(17)	C−O8×0.50(3)	1.36(6)
Sr3−O7×1.49(7)	2.845(19)	C−O9×0.50(3)	1.32(7)
		C−O10×1.00(3)	1.34(5)
Sr4−O6×2	2.590(16)	C−O11×1.00(3)	1.32(4)
Sr4−O7×1.49(7)	2.535(17)		
Sr4−O8×1.00(6)	2.835(14)	O8−C−O10×2.00(6)	111(6)
Sr4−O9×1.00(6)	2.807(18)	O10−C−O10×1.00(3)	137(6)
Sr4−O10×1.00(3)	2.52(3)	O9−C−O11×2.00(6)	117(6)
Sr4−O11×1.00(3)	2.50(2)	O11−C−O11×1.00(3)	127(4)

on the anionic sublattice, and that the quenching from 1123 K freezes this disorder, only allowing a mixture of these two configurations with a very short length of correlation within one configuration. Additionally, this RP_2^1 block exhibits $O_{5.87}$ stoichiometry, resulting in the aforementioned $CoO_{4.87}$ average polyhedron, which implies that tetrahedral coordination (reminiscent of the structure derived from brownmillerite[41]) locally occurs in the mixed configuration to adapt the actual anion deficiency.

Such a variety of cobalt environments should lead to a great positional disorder for oxygen, in agreement with the relatively large thermal displacement parameter of 4.4(6) Å^2 found for O3. Large thermal displacements correlated with this type of defect structure were also reported in $Sr_3Co_2O_{7-\delta}$,[39] for which the authors state that no split site model (i.e., displacement of the oxygen on a specific position, namely, O2 and O3, in the cited reference) can be applied; these authors indeed consider that the displacement directions and magnitudes are randomized by local interactions associated with the large defect concentration. Local superstructure spots were also observed in a similar system by Gillie et al.[40] upon SAED. It is therefore important to underline that the powder ND analysis was performed in a simple orthorhombic cell, selecting the most symmetric space group *Pmmm*. Because our ED study clearly showed the existence of local orderings at different levels of structure, the orientation of the carbonate groups and the distortion of the cobalt polyhedra through their connection are certainly factors that locally imply a larger unit cell with a different symmetry, not applied herein. As a result, the as-described structure of this new compound is an "average one".

dx.doi.org/10.1021/ic3026232 | *Inorg. Chem.* 2013, 52, 4977−4984

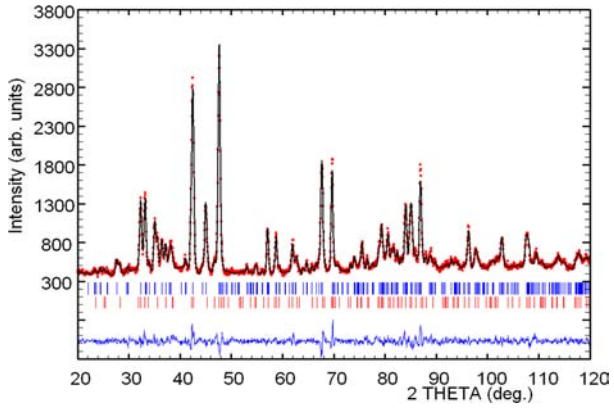

Figure 8. Experimental, calculated, and difference profiles for the powder ND data collected for the as-synthesized $Sr_7Co_4(CO_3)O_{11.36}$ sample at room temperature.

Considering the strongly lamellar character of the present framework, the structure can be described in terms of structural slices: rock salt, RS; perovskite, P; carbonate, SC. Along $\vec{c}$, the sequence of the stacked slices is

RS – P – P –RS – P – SC – P – …

RP^1_2 RP^1_1 S2CC

The structure can therefore be developed in terms of different members with two characteristics: each block contains at least one cobalt layer, and the cobalt layers belonging to different blocks are not directly connected along $\vec{c}$. Such a developed formulation allows one to easily identify, for example, the number of magnetic layers and the number of intergrown nonmagnetic blocks. According to this model, the parent structure $Sr_3Co_2O_{5.87}$ remains RP^1_2, whereas $Sr_4Co_2(CO_3)O_{5.49}$ is written as $[RP^1_1\text{-S2CC}]$, to be compared with RP^1_1 $LaSr_3Fe_3O_{10-\delta}$.[42]

Magnetic and Electronic Transport Properties. The resistivity was collected in the 200−400 K temperature range, under 0 and 7 T, from a freshly prepared sample. The compound shows a high resistivity with $p \sim 25\ \Omega$ cm at 390 K similar to that observed in cobalt oxides displaying a similar valence state (Figure 10). The linearity of the curve $\ln \rho = f(1/T)$ allows one to demonstrate a semiconducting behavior with an activation energy of 294 meV. Data collected at 7 T do not reveal magnetoresistance for that new cobalt oxycarbonate.

Magnetic susceptibility data, collected between 2 and 390 K, show a highly complex behavior between 2 and 300 K. Indeed,

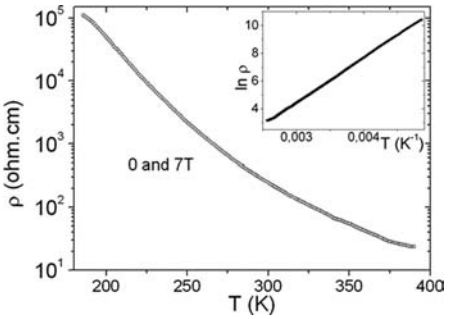

Figure 10. Resistivity measurement collected in the range 200−400 K, under 0 and 7 T.

four characterisitic temperatures can be defined. Upon cooling from 300 K, a first separation of zero-field-cooled (ZFC) and field-cooled (FC) curves occurs at 280 K, followed by a transition at 50 K. Between these two temperatures, two small accidents can be observed at 130 and 230 K (Figure 11). The

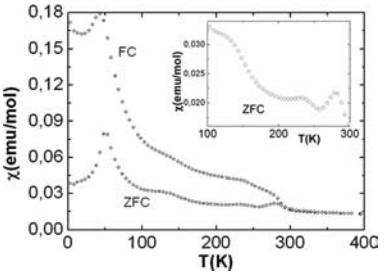

Figure 11. Magnetic susceptibility data collected between 2 and 390 K under 0.3 T.

opening of the ZFC−FC curves below 280 K can be associated with the presence of a weak ferromagnetic-like component, which can be confirmed by a small hysteresis loop observed at 275 K (Figure 12). At 5 K, the hysteresis loop is well opened, with a coercive field of ∼5 kOe and a remanent magnetization of 0.025 μ_B/mol of Co. This moment remains very weak compared to the values that can be obtained when the Co^{2+} and Co^{3+} high-spin magnetic moments are aligned (3 and 4 μ_B, respectively). These magnetic properties are typical of the results observed for RP_2 cobaltites with a cobalt valency close to 2.68, with several magnetic transitions.[23,38,39] The Curie−Weiss domain is not well established at 400 K, and no Curie−Weiss analysis can be performed. The complexity of the *T*-dependent magnetic behavior might be seen as a direct consequence of the complex crystal chemistry, involving the intergrowth of two RP

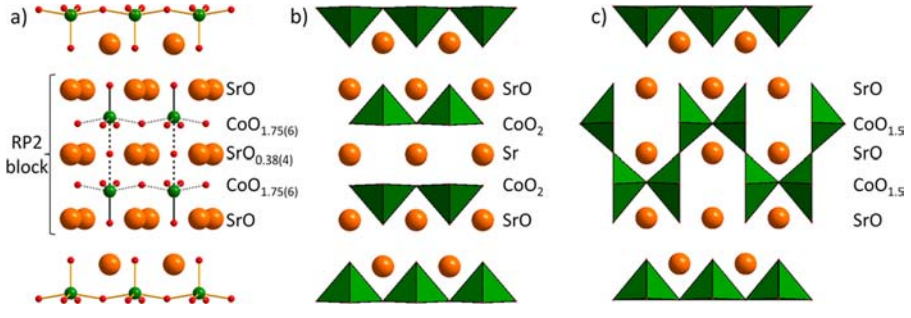

Figure 9. (a) Oxygen distribution at the level of the RP^1_2 block and two limit models for the CoO_5 pyramids with the basis (b) parallel and (c) perpendicular to the layer plane.

dx.doi.org/10.1021/ic3026232 | Inorg. Chem. 2013, 52, 4977−4984

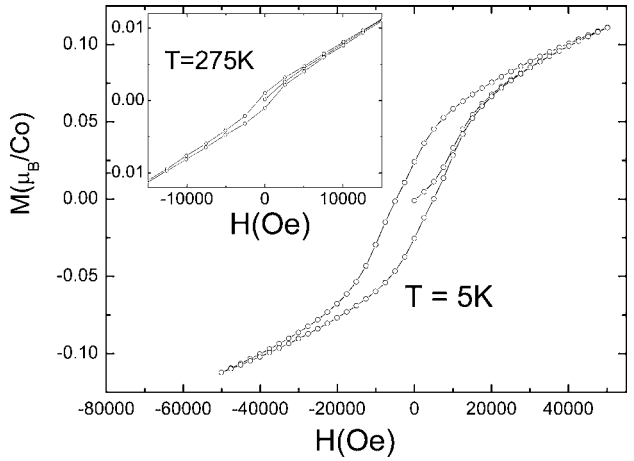

Figure 12. Magnetization loops measured at 275 K (inset) and 5 K.

layered structures coupled with structural disorder with respect to cobalt polyhedra, the presence of $Sr_4Co_2(CO_3)O_{6-\delta}$ as secondary phase detected from neutron analyses, and a possible beginning of reactivity with ambient air. A variable-temperature ND study would therefore be of interest to clarify this complex behavior.

CONCLUDING REMARKS

The new carbonated compound $Sr_7Co_4(CO_3)O_{11.36}$ exhibits an original structure, which can be most simply described as an intergrowth between one RP^1_2 block and one carbonated RP^1_3 block. Such a regular intergrowth has never been reported so far. This phase stabilization involves complex crystal chemistry mechanisms, including the partial carbon substitution for cobalt species in a RP host matrix and large oxygen nonstoichiometry. This peculiar structure goes along with a complex magnetic response and a semiconducting behavior typically observed in RP_1 or RP_2 members with cobalt valency close to 2.68. The ability of the RP^1_m series to form a regular intergrowth between two distinct members has been demonstrated in this paper owing to carbonated layer substitution for the magnetic cobalt layer. This opens the door to a large family of layered cobalt compounds, playing with each of the structural units, i.e., different RP^n_m members and other complex groups as S2CC including a part of no magnetic layers.

ASSOCIATED CONTENT

Supporting Information

Simulated ED patterns, application to $Sr_7Co_4(CO_3)O_{13-\delta}$, line-broadening analysis of isolated 00l reflections, and beam sensitivity of superstructure reflections. This material is available free of charge via the Internet at http://pubs.acs.org.

AUTHOR INFORMATION

Corresponding Author

*E-mail: denis.pelloquin@ensicaen.fr.

Notes

The authors declare no competing financial interest.

ACKNOWLEDGMENTS

The authors are grateful to Prof. M. Daturi for the IR measurements and fruitful discussions. This work was carried out under the framework of the MADBLAST project supported by the ANR (Grant ANR-09-BLAN-0187-01). This work was supported by the FP7 European Initial Training Network SOPRANO (Grant GA-2008-214040).

REFERENCES

(1) Ruddlesden, S. N.; Popper, P. *Acta Crystallogr.* **1958**, *11*, 54.
(2) Sawa, H.; Obara, K.; Akimitsu, J.; Matsui, Y.; Horiuchi, S. *J. Phys. Soc. Jpn.* **1989**, *58* (7), 2252−5.
(3) Michel, C.; Hervieu, M.; Borel, M. M.; Grangin, A.; Deslandes, F.; Provost, J.; Raveau, B. *Z. Phys. B* **1987**, *68*, 421.
(4) Babu, T. G. N.; Fish, D. J.; Greaves, C. *J. Mater. Chem.* **1991**, *1* (4), 677.
(5) Barnabe, A.; Letouze, F.; Pelloquin, D.; Maignan, A.; Hervieu, M.; Raveau, B. *Chem. Mater.* **1997**, *9* (10), 2205.
(6) Michel, C.; Letouze, F.; Martin, C.; Hervieu, M.; Raveau, B. *Phys. C: Supercond. (Amsterdam, The Netherlands)* **1996**, *262* (3 & 4), 159.
(7) Slater, P. R.; Greaves, C.; Slaski, M.; Muirhead, C. M. *Phys. C: Supercond. Its Appl. (Amsterdam, The Netherlands)* **1993**, *213* (1−2), 14.
(8) Cava, R. J.; Batlogg, B.; Van Dover, R. B.; Krajewski, J. J.; Waszczak, J. V.; Fleming, R. M.; Peck, W. F., Jr.; Rupp, L. W., Jr.; Marsh, P.; et al. *Nature (London, U.K.)* **1990**, *345* (6276), 602.
(9) Hiroi, Z.; Takano, M.; Azuma, M.; Takeda, Y. *Nature (London, U.K.)* **1993**, *364* (6435), 315.
(10) Kinoshita, K.; Shibata, H.; Yamada, T. *Phys. C: Supercond. Its Appl. (Amsterdam, The Netherlands)* **1991**, *176* (4−6), 433.
(11) Nguyen, N.; Choisnet, J.; Hervieu, M.; Raveau, B. *J. Solid State Chem.* **1981**, *39*, 120.
(12) Michel, C.; Raveau, B. *Rev. Chim. Miner.* **1984**, *21* (4), 407.
(13) Battle, P. D.; Blundell, S. J.; Green, M. A.; Hayes, W.; Honold, M.; Klehe, A. K.; Laskey, N. S.; Millburn, J. E.; Murphy, L.; et al. *J. Physics: Condens. Matter* **1996**, *8* (32), L427.
(14) Bader, S. D.; Osgood, R. C., III; Miller, D. J.; Mitchell, J. F.; Jiang, J. S. *J. Appl. Phys.* **1998**, *83* (11, Pt. 2), 6385.
(15) Moritomo, Y.; Tomioka, Y.; Asamitsu, A.; Tokura, Y.; Matsui, Y. *Phys. Rev. B: Condens. Matter* **1995**, *51* (5), 3297.
(16) Battle, P. D.; Green, M. A.; Lago, J.; Millburn, J. E.; Rosseinsky, M. J.; Vente, J. F. *Chem. Mater.* **1998**, *10* (2), 658.
(17) Maeda, H.; Tanaka, Y.; Fukutomi, M.; Asano, T. *Jpn. J. Appl. Phys., Part 2: Lett.* **1988**, *27* (2), L209.
(18) Sheng, Z. Z.; Hermann, A. M. *Nature (London, U.K.)* **1988**, *332* (6159), 55.
(19) Putilin, S. N.; Antipov, E. V.; Chmaissem, O.; Marezio, M. *Nature (London, U.K.)* **1993**, *362* (6417), 226.
(20) Karimoto, S.-I.; Naito, M. *Jpn. J. Appl. Phys., Part 2: Lett.* **1999**, *38* (3B), L283.
(21) Seshadri, R.; Martin, C.; Hervieu, M.; Raveau, B.; Rao, C. N. R. *Chem. Mater.* **1997**, *9*, 270.
(22) Moritomo, Y.; Asamitsu, A.; Kuwahara, H.; Tokura, Y. *Nature* **1996**, *380*, 141.
(23) Demont, A.; Pelloquin, D.; Hebert, S.; Breard, Y.; Hoewing, J.; Miyazaki, Y.; Maignan, A. *J. Solid State Chem.* **2011**, *184* (7), 1655.
(24) Demont, A.; Breard, Y. D.; Hebert, S.; Pelloquin, D.; Maignan, A. *Chem. Mater.* **2012**, submitted for publication.
(25) Hervieu, M.; Pelloquin, D.; Michel, C.; Van Tendeloo, G.; Raveau, B. *J. Solid State Chem.* **1994**, *112* (1), 139.
(26) Maignan, A.; Pelloquin, D.; Malo, S.; Michel, C.; Hervieu, M.; Raveau, B. *Phys. C: Supercond. (Amsterdam, The Netherlands)* **1995**, *249* (3&4), 220.
(27) Pelloquin, D.; Barrier, N.; Maignan, A.; Caignaert, V. *Solid State Sci.* **2005**, *7*, 853.
(28) Roisnel, T.; Rodriguez-Carvajal, J. *Mater. Sci. Forum* **2001**, *378−381*, 118−123 (EPDIC 7, Part 1)..
(29) (a) Van Tendeloo, G.; Van Dyck, D.; Kuypers, S.; Zandbergen, H. W.; Amelinckx, S. *Phys. Status Solidi A: Appl. Res.* **1987**, *102* (2), 597. (b) Pelloquin, D.; Caldes, M. T.; Maignan, A.; Michel, C.; Hervieu, M.; Raveau, B. *Phys. C* **1993**, *208* (1 & 2), 121.
(30) Milat, O.; Van Tendeloo, G.; Amelinckx, S.; Babu, T. G. N.; Greaves, C. *J. Solid State Chem.* **1994**, *109* (1), 5.

(31) Domenges, B.; Hervieu, M.; Raveau, B. *Phys. C: Supercond. Its Appl. (Amsterdam, The Netherlands)* **1993**, *207* (1−2), 65.
(32) Huve, M.; Michel, C.; Maignan, A.; Hervieu, M.; Martin, C.; Raveau, B. *Phys. C: Supercond. Its Appl. (Amsterdam, The Netherlands)* **1993**, *205* (3−4), 219.
(33) Bréard, Y.; Michel, C.; Hervieu, M.; Raveau, B. *J. Mater. Chem.* **2000**, *10*, 1043.
(34) Bréard, Y.; Michel, C.; Hervieu, M.; Nguyen, N.; Ducouret, A.; Hardy, V.; Maignan, A.; Raveau, B.; Bouree, F.; Andre, G. *Chem. Mater.* **2004**, *16* (15), 2895.
(35) Yamaura, K.; Huang, Q.; Lynn, J. W.; Erwin, R. W.; Cava, R. J. *J. Solid State Chem.* **2000**, *152* (2), 374.
(36) Miyazaki, Y.; Yamane, H.; Kajitani, T.; Oku, T.; Hiraga, K.; Morii, Y.; Fuchizaki, F.; Funahashi, S.; Hirai, T. *Phys. C: Supercond. Its Appl. (Amsterdam, The Netherlands)* **1992**, *191*, 434.
(37) Dann, S. E.; Weller, M. T. *J. Solid State Chem.* **1995**, *115* (2), 499.
(38) Viciu, L.; Zandbergen, H. W.; Xu, Q.; Huang, Q.; Lee, M.; Cava, R. J. *J. Solid State Chem.* **2006**, *179* (2), 500.
(39) Hill, J. M.; Dabrowski, B.; Mitchell, J. F.; Jorgensen, J. D. *Phys. Rev. B: Condens. Matter Mater. Phys.* **2006**, *74* (17).
(40) Gillie, L. J.; Hadermann, J.; Hervieu, M.; Maignan, A.; Martin, C. *Chem. Mater.* **2008**, *20* (19), 6231.
(41) Mitchell, R. H. *Perovskites: Modern and Ancient*; Almaz Press Inc.: Ontario, Canada, 2002.
(42) Lee, J. Y.; Swinnea, J. S.; Steinfink, H.; Reiff, W. M.; Pei, S.; Jorgensen, J. D. *J. Solid State Chem.* **1993**, *103* (1), 1−15.

dx.doi.org/10.1021/ic3026232 | *Inorg. Chem.* 2013, 52, 4977−4984